XIV International Conference on Computational Plasticity. Fundamentals and Applications
COMPLAS XIV
E. Oñate, D.R.J. Owen, D. Peric & M. Chiumenti (Eds)

MULTI-FIELD MODELLING AND SIMULATION OF LARGE DEFORMATION DUCTILE FRACTURE

M. DITTMANN[*], C. HESCH[*], J. SCHULTE[*], F. ALDAKHEEL[†] AND M. FRANKE[#]

[*] Chair of Computational Mechanics
University of Siegen
Paul-Bonatz-Straße 9-11, 57068 Siegen, Germany
e-mail: maik.dittmann@uni-siegen.de, christian.hesch@uni-siegen.de,
web page: https://www.mb.uni-siegen.de/nm

[†] Institute of Applied Mechanics
University of Stuttgart
Pfaffenwaldring 7, 70569 Stuttgart, Germany
e-mail: fadi.aldakheel@mechbau.uni-stuttgart.de,
web page: http://www.mechbau.uni-stuttgart.de/ls1

[#] Institute of Mechanics
Karlsruhe Institute of Technology
Otto-Ammann-Platz 9, 76131 Karlsruhe, Germany
e-mail: marlon.franke@kit.edu
web page: https://www.ifm.kit.edu

Key words: Ductile Fracture, Large Deformation, Phase-field, Contact mechanics

Abstract. In the present contribution we focus on a phase-field approach to ductile fracture applied to large deformation contact problems. Phase-field approaches to fracture allow for an efficient numerical investigation of complex three-dimensional fracture problems, as they arise in contact and impact situations. To account for large deformations the underlying formulation is based on a multiplicative decomposition of the deformation gradient into an elastic and plastic part. Moreover, we make use of a fourth-order crack regularization combined with gradient plasticity. Eventually, a demonstrative example shows the capability of the proposed framework.

1 INTRODUCTION

The numerical investigation of fracture using phase-field approaches has gained increasing attention in the last decade, see Miehe et al. [1] and Kuhn and Müller [2]. In contrast to the costly and complex computational modeling of sharp cracks, the formulation in this works is based on the introduction of a diffusive interface, see also Weinberg and Hesch [3] for a detailed investigation on Allen-Cahn type as well as Cahn-Hilliard type equations.

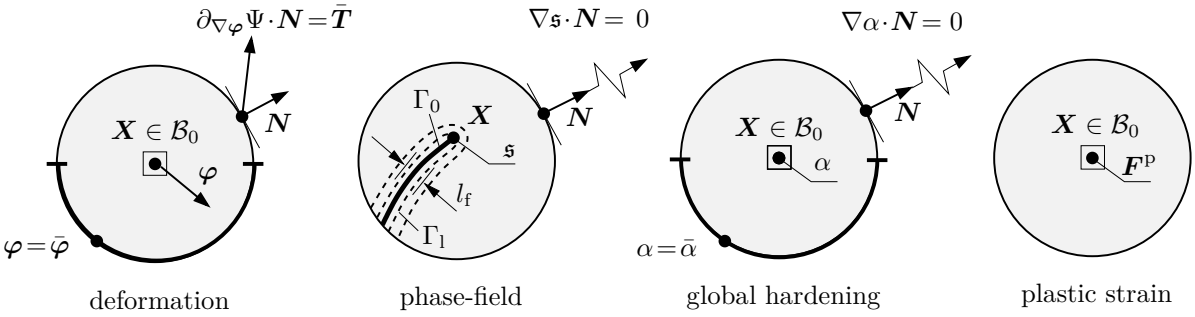

Figure 1: Primary fields of inelastic deformable solids coupled with phase field fracture.

The assumption that the material fails locally upon the attainment of a specific fracture energy as introduced by Francfort and Marigo [4] and Bourdin et al. [5], allows to formulate a variational statement for brittle fracture, see e.g. Karma et al. [6]. An extension to large deformations relying on a multiplicative decomposition of the deformation gradient into a compressive and a tensile part along with a structure preserving time integration scheme is given in Hesch and Weinberg [7], whereas adaptations to ductile fracture have recently proposed in e.g. Aldakheel [8], Miehe et al. [9] and Borden et al. [10]. The formulations introduced therein are able to predict fracture in ductile solids which undergoes large elastic and/or plastic deformations. In addition, the application of a phase-field fracture approach to contact and impact problems was recently proposed in Hesch et al. [11] and Dittmann et al. [12].

The purpose of the present contribution is to introduce a framework for the simulation of ductile fracture within large deformation contact and impact situations. Therefore, we combine a nonlinear elastoplastic formulation based on a multiplicative decomposition of the deformation gradient with a fourth order phase-field formulation and gradient plasticity. Eventually, we apply the proposed approach along with a frictional mortar contact formulation and demonstrate the capability on a representative example.

2 GOVERNING EQUATIONS

Let $\mathcal{B}_0 \subset \mathbb{R}^n$ with $n \in \{2,3\}$ be the reference configuration of the body of interest. The proposed multi-field approach to phase-field-type crack propagation in inelastic deformable solids is described by the following primary fields of the coupled problem:

- The *deformation map* $\boldsymbol{\varphi}$ which maps at time $t \in \mathcal{T}$ points $\boldsymbol{X} \in \mathcal{B}_0$ of the reference configuration $\mathcal{B}_0$ onto points $\boldsymbol{x} \in \mathcal{B}_t$ of the current configuration $\mathcal{B}_t$

$$\boldsymbol{\varphi}(\boldsymbol{X}) : \mathcal{B}_0 \times \mathcal{T} \to \mathbb{R}^n \quad \text{with} \quad \boldsymbol{x} = \boldsymbol{\varphi}(\boldsymbol{X}, t) \tag{1}$$

  as depicted in Figure 1a. The material deformation gradient is defined by $\boldsymbol{F} := \nabla\boldsymbol{\varphi}(\boldsymbol{X})$ with $J := \det[\boldsymbol{F}] > 0$.

- The *crack phase-field* $\mathfrak{s}$ is interpreted as an auxiliary variable that approximates the sharp crack topology. It defines a regularized crack surface functional $\Gamma_l(\mathfrak{s})$ that

converges in the limit $l_{\mathrm{f}} \to 0$ to the sharp crack surface Γ_0

$$\mathfrak{s}(\boldsymbol{X}, t) : \mathcal{B}_0 \times \mathcal{T} \to \mathbb{R}, \quad \text{with} \quad \mathfrak{s} \in [0, 1] \quad \text{and} \quad \dot{\mathfrak{s}} \geq 0 \tag{2}$$

as indicated in Figure 1b, where the value $\mathfrak{s}(\boldsymbol{X}, t) = 0$ refers to the unbroken and $\mathfrak{s}(\boldsymbol{X}, t) = 1$ to the fully broken state of the material. The crack growth creates a new internal boundary $\Gamma_0^{\mathrm{cr}}(t) \subset \mathbb{R}^{n-1}$ based on energetic criterion. Here, the total energy within the sharp crack interface E^{cr} is approximated based on a crack surface density function γ resulting with a regularized crack interface as

$$\int_{\Gamma_0^{\mathrm{cr}}} g_{\mathrm{c}} \, \mathrm{d}\Gamma \approx \int_{\mathcal{B}_0} g_{\mathrm{c}} \gamma \, \mathrm{d}V \quad \text{with} \quad \gamma(\mathfrak{s}, \nabla\mathfrak{s}, \Delta\mathfrak{s}) = \frac{1}{4 l_{\mathrm{f}}} \mathfrak{s}^2 + \frac{l_{\mathrm{f}}}{2} \nabla\mathfrak{s} \cdot \nabla\mathfrak{s} + \frac{l_{\mathrm{f}}^3}{4} (\Delta\mathfrak{s})^2 \tag{3}$$

g_{c} is the Griffith-type critical energy release rate and l_{f} is the fracture length scale.

- The long-range micro-motion field α denoted as the global hardening variable

$$\alpha(\boldsymbol{X}, t) : \mathcal{B}_0 \times \mathcal{T} \to \mathbb{R} \quad \text{with} \quad \alpha = \bar{\alpha} \text{ on } \partial\mathcal{B}_0^{\alpha_{\mathrm{d}}} \quad \text{and} \quad \nabla\alpha \cdot \boldsymbol{N} = 0 \text{ on } \partial\mathcal{B}^{\alpha_{\mathrm{n}}} \tag{4}$$

illustrated in Figure 1c, where the gradient $\nabla\alpha(\boldsymbol{X}, t)$ is governed by a *plastic length scale* l_{p} that accounts for nonlocal hardening effects. Following the recent work Miehe et al. [14], the fracture length scale is $l_{\mathrm{f}} \leq l_{\mathrm{p}}$ to ensures that the damage zones of ductile fracture are inside of plastic zones.

- The short range micro-motion field $\boldsymbol{F}^{\mathrm{p}}$ denoted as the plastic deformation map

$$\boldsymbol{F}^{\mathrm{p}}(\boldsymbol{X}, t) : \mathcal{B}_0 \times \mathcal{T} \to \mathbb{R}^{n \times n}, \quad \det[\boldsymbol{F}^{\mathrm{p}}] = 1, \tag{5}$$

is locally defined and not constrained by boundary conditions, see Figure 1d.

The subsequent constitutive approach to phase-field ductile fracture focuses on the set

$$\mathfrak{C} := \{\nabla\boldsymbol{\varphi}, \boldsymbol{F}^{\mathrm{p}}, \alpha, \nabla\alpha, \mathfrak{s}, \nabla\mathfrak{s}, \Delta\mathfrak{s}\} \, , \tag{6}$$

2.1 Evolution of the Regularized Crack Surface Topology

Following the recent work of Miehe et al. [9], the rate of the work needed to create a diffusive fracture topology is driven by constitutive functions, postulating a global evolution equation of regularized crack surface

$$\dot{E}^{\mathrm{cr}} = \int_{\mathcal{B}_0} g_{\mathrm{c}} \, \delta_{\mathfrak{s}} \widehat{\gamma}(\mathfrak{s}, \nabla\mathfrak{s}, \Delta\mathfrak{s}) \, \dot{\mathfrak{s}} \, \mathrm{d}V = \int_{\mathcal{B}_0} \Big[\mathcal{H} - \mathcal{R} \Big] \, \dot{\mathfrak{s}} \, \mathrm{d}V \tag{7}$$

Here, $\mathcal{H}$ is the crack driving force defined in (27) and $\mathcal{R} = \eta_{\mathrm{f}} \, \dot{\mathfrak{s}}$ is a viscous crack resistance, where $\eta_{\mathrm{f}} \geq 0$ is a material parameter which characterize viscosity of the crack propagation. The functional derivative of the crack density function is defined as

$$\delta_{\mathfrak{s}} \widehat{\gamma}(\mathfrak{s}, \nabla\mathfrak{s}, \Delta\mathfrak{s}) := \partial_{\mathfrak{s}} \widehat{\gamma} - \mathrm{Div}[\partial_{\nabla\mathfrak{s}} \widehat{\gamma}] + \Delta[\partial_{\Delta\mathfrak{s}} \widehat{\gamma}] \, . \tag{8}$$

Then equation (7) gives the crack phase field evolution as a generalized Ginzburg-Landau-type structure

$$\eta_{\mathrm{f}}\,\dot{\mathfrak{s}} = \mathcal{H} - g_{\mathrm{c}}\left[\frac{1}{2l_{\mathrm{f}}}\,\mathfrak{s} - l_{\mathrm{f}}\Delta\mathfrak{s} + \frac{l_{\mathrm{f}}^3}{2}\,\Delta\Delta\mathfrak{s}\right] , \tag{9}$$

along with the Neumann-type boundary conditions

$$\nabla(l_{\mathrm{f}}^2\Delta\mathfrak{s} - \mathfrak{s})\cdot\boldsymbol{N} = 0 \text{ on } \partial\mathcal{B}_0^{\mathfrak{s}_{\mathrm{n}}} \quad \text{and} \quad \Delta\mathfrak{s}\cdot\boldsymbol{N} = 0 \text{ on } \partial\mathcal{B}_0^{\mathfrak{s}_{\mathrm{n}}} , \tag{10}$$

where the expression $\Delta\Delta\mathfrak{s} = \mathrm{Div}[\mathrm{Div}[\nabla^2\mathfrak{s}]]$ is the Bi-Laplacian of the crack phase field. Based on thermodynamical arguments, we demand irreversible crack evolution $\dot{E}^{\mathrm{cr}} \geq 0$, as discussed in the work of Miehe et al. [1, 9]. This global irreversibility constraint of crack evolution is satisfied by ensuring a positive evolution of the crack phase field as

$$\dot{\mathfrak{s}} = \frac{1}{\eta_{\mathrm{f}}}\left\langle \mathcal{H} - g_{\mathrm{c}}\left[\frac{1}{2l_{\mathrm{f}}}\,\mathfrak{s} - l_{\mathrm{f}}\Delta\mathfrak{s} + \frac{l_{\mathrm{f}}^3}{2}\,\Delta\Delta\mathfrak{s}\right]\right\rangle \geq 0 , \tag{11}$$

where $\langle x\rangle := (x + |x|)/2$ is the McAuley bracket.

2.2 Coupling Gradient Plasticity to Gradient Damage Mechanics

In large strain context, the deformation gradient is given by a multiplicative decomposition into elastic and plastic parts $\boldsymbol{F} = \boldsymbol{F}^{\mathrm{e}}\boldsymbol{F}^{\mathrm{p}}$. Then, an elastic deformation measure is the *contra-variant Eulerian elastic Finger tensor* $\boldsymbol{b}^{\mathrm{e}} = \boldsymbol{F}^{\mathrm{e}}(\boldsymbol{F}^{\mathrm{e}})^{\mathrm{T}}$ that provides the definition

$$\boldsymbol{b}^{\mathrm{e}} = \boldsymbol{F}(\boldsymbol{C}^{\mathrm{p}})^{-1}\boldsymbol{F}^{\mathrm{T}} \quad \text{with} \quad \boldsymbol{C}^{\mathrm{p}} = (\boldsymbol{F}^{\mathrm{p}})^{\mathrm{T}}\boldsymbol{F}^{\mathrm{p}} . \tag{12}$$

The kinematic basis for a decoupling of the constitutive response into volumetric elastic and isochoric elastic-plastic contributions is

$$\boldsymbol{b}^{\mathrm{e}} = J^{2/3}\bar{\boldsymbol{b}}^{\mathrm{e}} \tag{13}$$

which defines the volumetric and isochoric parts

$$J = \det[\boldsymbol{F}] = \det[\boldsymbol{F}^{\mathrm{e}}\boldsymbol{F}^{\mathrm{p}}] = \det[\boldsymbol{F}^{\mathrm{e}}] = J^{\mathrm{e}} \quad \text{and} \quad \bar{\boldsymbol{b}}^{\mathrm{e}} = J^{-2/3}\boldsymbol{F}(\boldsymbol{C}^{\mathrm{p}})^{-1}\boldsymbol{F}^{\mathrm{T}} . \tag{14}$$

The storage energy function $\widehat{\Psi}$ is assumed to depend on the array $\mathfrak{C}$ of constitutive state variables introduced in (6) as

$$\widehat{\Psi}(\mathfrak{C}) = \widehat{\Psi}^{\mathrm{e}}(\boldsymbol{b}^{\mathrm{e}};\mathfrak{s}) + \widehat{\Psi}^{\mathrm{p}}(\alpha,\nabla\alpha) . \tag{15}$$

Here, the phase field $\mathfrak{s}$ enters the constitutive functions as a generalized internal variable. However, it is considered as a geometric property that models a regularized crack surface. The elastic contributions are given by

$$\begin{aligned}\widehat{\Psi}^{\mathrm{e}} &= g_{\mathrm{vol}}(\mathfrak{s})\widehat{\Psi}^{\mathrm{e}}_{\mathrm{vol}}(J) + g_{\mathrm{dev}}(\mathfrak{s})\widehat{\Psi}^{\mathrm{e}}_{\mathrm{dev}}(\bar{\boldsymbol{b}}^{\mathrm{e}}) \\ &= \frac{\kappa}{2}g_{\mathrm{vol}}(\mathfrak{s})(J-1)^2 + \frac{\mu}{2}g_{\mathrm{dev}}(\mathfrak{s})(\mathrm{tr}[\bar{\boldsymbol{b}}^{\mathrm{e}}] - 3)\end{aligned} \tag{16}$$

in terms of the volumetric and isochoric degradation functions defined as

$$g_{\mathrm{vol}}(\mathfrak{s}) = \begin{cases} g(\mathfrak{s}) & J > 1 \\ 1 & J \leq 1 \end{cases} \quad \text{and} \quad g_{\mathrm{dev}}(\mathfrak{s}) = g(\mathfrak{s}), \tag{17}$$

where $g(\mathfrak{s}) = a_{\mathrm{g}}((1-\mathfrak{s})^3 - (1-\mathfrak{s})^2) - 2(1-\mathfrak{s})^3 + 3(1-\mathfrak{s})^2$ with $a_{\mathrm{g}} \geq 0$. Next, we introduce the constitutive relation related to the Kirchhoff stress as

$$\boldsymbol{\tau} = 2\frac{\partial \widehat{\Psi}^{\mathrm{e}}}{\partial \boldsymbol{b}^{\mathrm{e}}}\boldsymbol{b}^{\mathrm{e}} = \boldsymbol{\tau}_{\mathrm{vol}} + \boldsymbol{\tau}_{\mathrm{dev}} \tag{18}$$

with the volumetric and isochoric stress parts defined as

$$\boldsymbol{\tau}_{\mathrm{vol}} = \kappa g_{\mathrm{vol}}(\mathfrak{s})(J^2 - J)\boldsymbol{I} \quad \text{and} \quad \boldsymbol{\tau}_{\mathrm{dev}} = \mu g_{\mathrm{dev}}(\mathfrak{s})\mathrm{dev}[\bar{\boldsymbol{b}}^{\mathrm{e}}]. \tag{19}$$

The plastic contribution is decomposed into local and gradient parts. For the modeling of length scale effects in isotropic gradient plasticity, we focus on the equivalent plastic strain α and its gradient $\nabla\alpha$. It is assumed to have the form

$$\widehat{\Psi}^{\mathrm{p}}(\alpha, \nabla\alpha) = \int_0^{\alpha} \widehat{y}(\tilde{\alpha})\,\mathrm{d}\tilde{\alpha} + y_0\frac{l_p^2}{2}\|\nabla\alpha\|^2, \tag{20}$$

where $l_p \geq 0$ is a plastic length scale related to a strain-gradient hardening effect. $\widehat{y}(\alpha)$ is an isotropic local hardening function obtained form homogeneous experiments. We use in what follows the saturation-type function

$$\widehat{y}(\alpha) = y_0 + (y_\infty - y_0)(1 - \exp[-\eta\alpha]) + h\alpha \tag{21}$$

widely used in metal plasticity, in terms of the four material parameters $y_0 > 0$, $y_\infty \geq y_0$, $\eta > 0$ and $h \geq 0$, where the initial yield stress y_0 determines the threshold of the effective elastic response. Next, we define the dissipation energy *locally* as the difference of the external stress power and the evolution of the energy storage, by the standard Clausius-Planck inequality

$$\mathcal{D} = \boldsymbol{\tau} : \boldsymbol{d} - \frac{\mathrm{d}}{\mathrm{d}t}\widehat{\Psi}^{\mathrm{e}} \geq 0, \tag{22}$$

where the rate of the deformation tensor $\boldsymbol{d}$ is the symmetric part of the spatial velocity gradient $\boldsymbol{l} = \dot{\boldsymbol{F}}\boldsymbol{F}^{-1}$. Moreover, the rate of change of the energy storage reads

$$\frac{\mathrm{d}}{\mathrm{d}t}\widehat{\Psi}^{\mathrm{e}} = \frac{\partial \widehat{\Psi}^{\mathrm{e}}}{\partial \boldsymbol{b}^{\mathrm{e}}} : \dot{\boldsymbol{b}}^{\mathrm{e}} + \frac{\partial \widehat{\Psi}^{\mathrm{e}}}{\partial \mathfrak{s}}\dot{\mathfrak{s}}, \tag{23}$$

the evolution of the elastic storage energy function can be expressed in terms of the material time derivative

$$\dot{\boldsymbol{b}}^{\mathrm{e}} = \boldsymbol{l}\boldsymbol{b}^{\mathrm{e}} + \boldsymbol{b}^{\mathrm{e}}\boldsymbol{l}^{\mathrm{T}} + \boldsymbol{F}(\dot{\boldsymbol{C}}^{\mathrm{p}})^{-1}\boldsymbol{F}^{\mathrm{T}}, \quad \dot{\boldsymbol{C}}^{\mathrm{p}} = (\dot{\boldsymbol{F}}^{\mathrm{p}})^{\mathrm{T}}\boldsymbol{F}^{\mathrm{p}} + (\boldsymbol{F}^{\mathrm{p}})^{\mathrm{T}}\dot{\boldsymbol{F}}^{\mathrm{p}}. \tag{24}$$

In case of isotropy, the skew-symmetric part of the spatial velocity gradient vanishes, i.e. $\boldsymbol{l} = \boldsymbol{d}$, and $\partial_{\boldsymbol{b}^{\mathrm{e}}} \widehat{\Psi}^{\mathrm{e}}$ commutes with $\boldsymbol{b}^{\mathrm{e}}$ such that the first term in (23) can be written as

$$\begin{aligned} \frac{\partial \widehat{\Psi}^{\mathrm{e}}}{\partial \boldsymbol{b}^{\mathrm{e}}} : \dot{\boldsymbol{b}}^{\mathrm{e}} &= \left[\frac{\partial \widehat{\Psi}^{\mathrm{e}}}{\partial \boldsymbol{b}^{\mathrm{e}}} \boldsymbol{b}^{\mathrm{e}}\right] : \boldsymbol{d} + \left[\boldsymbol{b}^{\mathrm{e}} \frac{\partial \widehat{\Psi}^{\mathrm{e}}}{\partial \boldsymbol{b}^{\mathrm{e}}}\right] : \boldsymbol{d} + \left[\frac{\partial \widehat{\Psi}^{e}}{\partial \boldsymbol{b}^{\mathrm{e}}} \boldsymbol{b}^{\mathrm{e}}\right] : [\boldsymbol{F}(\dot{\boldsymbol{C}}^{\mathrm{p}})^{-1} \boldsymbol{F}^{\mathrm{T}} (\boldsymbol{b}^{\mathrm{e}})^{-1}] \\ &= \left[2 \frac{\partial \widehat{\Psi}^{\mathrm{e}}}{\partial \boldsymbol{b}^{\mathrm{e}}} \boldsymbol{b}^{\mathrm{e}}\right] : [\boldsymbol{d} - \boldsymbol{d}^{\mathrm{p}}], \end{aligned} \tag{25}$$

where $\boldsymbol{d}^{\mathrm{p}} = -\frac{1}{2} \boldsymbol{F}(\dot{\boldsymbol{C}}^{\mathrm{p}})^{-1} \boldsymbol{F}^{\mathrm{T}} (\boldsymbol{b}^{\mathrm{e}})^{-1}$ is the Eulerian plastic rate of deformation tensor. With the Kirchoff stress we obtain the dissipation in the more explicit form

$$\mathcal{D} = \boldsymbol{\tau} : \boldsymbol{d}^{\mathrm{p}} + \mathcal{H} \dot{\mathfrak{s}}. \tag{26}$$

Therein, the former terms represent the plastic part of dissipation and the latter term is the fracture part of dissipation. Here, we introduced per definition the energetic driving force for the fracture phase-field $\mathcal{H}$ as

$$\mathcal{H} = -\partial_{\mathfrak{s}} \widehat{\Psi}^{\mathrm{e}}. \tag{27}$$

Regarding to the plastic material behavior, we postulate a von Mises type plastic yield function as

$$\widehat{\Phi}^{\mathrm{p}}(\boldsymbol{\tau}, r^{\mathrm{p}}) = \|\boldsymbol{\tau}_{\mathrm{dev}}\| - \sqrt{\frac{2}{3}} r^{\mathrm{p}} \tag{28}$$

in terms of the dissipative resistance force r^{p} dual to the hardening variable α defined by the variational derivative of $\widehat{\Psi}^{\mathrm{p}}$ by α as

$$r^{\mathrm{p}} := \delta_{\alpha} \widehat{\Psi}^{\mathrm{p}} = \partial_{\alpha} \widehat{\Psi}^{\mathrm{p}} - \mathrm{Div}[\partial_{\nabla \alpha} \widehat{\Psi}^{\mathrm{p}}] \tag{29}$$

reflecting the characteristics of the gradient-extended plasticity model under consideration. A plastic Lagrange multiplier λ^{p} can introduced to enforce the Karush-Kuhn-Tucker conditions

$$\lambda^{\mathrm{p}} \geq 0, \quad \widehat{\Phi}^{\mathrm{p}} \leq 0, \quad \lambda^{\mathrm{p}} \widehat{\Phi}^{\mathrm{p}} = 0. \tag{30}$$

An extended dissipation potential can now be defined for the constrained optimization problem based on the concept of maximum dissipation

$$\widehat{V}(\dot{\mathfrak{C}}) = \underbrace{\sup}_{\boldsymbol{\tau}, r^{\mathrm{p}}} \underbrace{\sup}_{\lambda^{\mathrm{p}}} \left[\boldsymbol{\tau} : \boldsymbol{d}^{\mathrm{p}} - r^{\mathrm{p}} \dot{\alpha} - \lambda^{\mathrm{p}} \widehat{\Phi}^{\mathrm{p}}(\boldsymbol{\tau}, r^{\mathrm{p}})\right], \tag{31}$$

where the Lagrange parameter λ^{p} control the non-smooth evolution of the plasticity. This allows us to define the associated plastic evolution equations as follows

$$\boldsymbol{d}^{\mathrm{p}} = \lambda^{\mathrm{p}} \frac{\partial \widehat{\Phi}^{\mathrm{p}}}{\partial \boldsymbol{\tau}} = \lambda^{\mathrm{p}} \boldsymbol{n} \quad \text{and} \quad \dot{\alpha} = -\lambda^{\mathrm{p}} \frac{\partial \widehat{\Phi}^{\mathrm{p}}}{\partial r^{\mathrm{p}}}, \tag{32}$$

along with the loading-unloading condition introduced in (30). The evolution of the plastic deformation can be reformulated as

$$(\dot{\boldsymbol{C}}^{\mathrm{p}})^{-1} = -2\lambda^{\mathrm{p}} \boldsymbol{F}^{-1} \boldsymbol{n} \boldsymbol{b}^{\mathrm{e}} \boldsymbol{F}^{-\mathrm{T}} \tag{33}$$

To calculate the Lagrange multiplier, a penalty regularization can be utilized as follows

$$\lambda^{\mathrm{p}} = \frac{3}{2\eta_p} \left\langle \widehat{\Phi}^{\mathrm{p}}(\boldsymbol{\tau}, r^{\mathrm{p}}) \right\rangle \geq 0, \tag{34}$$

such that we obtain

$$\widehat{V}(\dot{\mathfrak{C}}) = \underbrace{\sup}_{\boldsymbol{\tau}, r^{\mathrm{p}}} \left[\boldsymbol{\tau} : \boldsymbol{d}^{\mathrm{p}} - r^{\mathrm{p}} \dot{\alpha} - \frac{3}{4\eta_{\mathrm{p}}} \left\langle \widehat{\Phi}^{\mathrm{p}}(\boldsymbol{\tau}, r^{\mathrm{p}}) \right\rangle^2 \right] . \tag{35}$$

This approach can be interpreted physically as a viscous regularization function. η_{p} is an additional material parameter which characterize viscosity of the plastic deformation.

The time integration of the plastic evolution equations is performed by a backward Euler scheme that leads to the construction of a return-mapping algorithm (see e.g. Simo and Hughes [13]) which is outlined in the following. For each time interval $[t_n, t_{n+1}]$ we assume the state at time t_n and the time step size $\Delta t = t_{n+1} - t_n$ are known. Furthermore we assume a trial state based on a purely elastic deformation and obtain the following trial variables

$$\begin{aligned} \boldsymbol{b}^{\mathrm{e}}_{\mathrm{tr}} &= \boldsymbol{F}_{n+1} (\boldsymbol{C}^{\mathrm{p}})^{-1}_{n} \boldsymbol{F}^{\mathrm{T}}_{n+1} \,, \\ \boldsymbol{\tau}_{\mathrm{dev,tr}} &= \mu g_{\mathrm{dev}}(\mathfrak{s}) \mathrm{dev}[\bar{\boldsymbol{b}}^{\mathrm{e}}_{\mathrm{tr}}] \,, \\ \boldsymbol{n}_{\mathrm{tr}} &= \frac{\boldsymbol{\tau}_{\mathrm{dev,tr}}}{\|\boldsymbol{\tau}_{\mathrm{dev,tr}}\|} \,, \\ \widehat{\Phi}^{p}_{\mathrm{tr}} &= \|\boldsymbol{\tau}_{\mathrm{dev,tr}}\| - \sqrt{\frac{2}{3}} r^{\mathrm{p}}_{n} \,, \end{aligned} \tag{36}$$

where $(\bullet)_n$, $(\bullet)_{n+1}$ and $(\bullet)_{\mathrm{tr}}$ denote the value of a given physical quantity for the respective state. A simplified time integration of (33) with the backward Euler scheme leads to

$$(\boldsymbol{C}^{\mathrm{p}}_{n+1})^{-1} = (\boldsymbol{C}^{\mathrm{p}}_{n})^{-1} - \frac{2}{3} \Delta t \lambda^{\mathrm{p}}_{n+1} \mathrm{tr}[\boldsymbol{b}^{\mathrm{e}}_{\mathrm{tr}}] \boldsymbol{F}^{-1}_{n+1} \boldsymbol{n}_{\mathrm{tr}} \boldsymbol{F}^{-\mathrm{T}}_{n+1} \tag{37}$$

supplemented by

$$\alpha_{n+1} = \alpha_n + \sqrt{\frac{2}{3}} \Delta t \lambda^{\mathrm{p}}_{n+1}. \tag{38}$$

If $\widehat{\Phi}^{\mathrm{p}}_{\mathrm{tr}} \leq 0$, then the process is purely elastic and the elastic trial state is the solution, i.e $\lambda^{\mathrm{p}}_{n+1} = 0$. If, on the other hand $\widehat{\Phi}^{\mathrm{p}}_{\mathrm{tr}} > 0$, then the trial state is not admissible and a plastic correction is needed.

$$\lambda^{\mathrm{p}}_{n+1} = \frac{3}{2\eta_{\mathrm{p}}} \left\langle \widehat{\Phi}^{\mathrm{p}}_{n+1} \right\rangle = \frac{3}{2\eta_{\mathrm{p}}} \left\langle \|\boldsymbol{\tau}_{\mathrm{dev},n+1}\| - \sqrt{\frac{2}{3}} r^{\mathrm{p}}_{n+1} \right\rangle \tag{39}$$

Because of the simplifications regarding the time integration of $\boldsymbol{C}^{\mathrm{p}}$ in (37), the incompressibility of the plastic deformation is not preserved. As a correction, we apply the return-map update only onto the deviatoric part of $\boldsymbol{C}^{\mathrm{p}}$ and make additionally use of the constraint $\det(\bar{\boldsymbol{b}}^{\mathrm{e}}_{n+1}) = 1$, see Borden et al. [10] for more details.

2.3 Contact formulation

Assuming that multiple bodies i are in contact, the boundary of the mechanical field is subdivided into Dirichlet, Neumann and contact boundaries

$$\partial\mathcal{B}_0^{(i),\varphi} \cup \partial\mathcal{B}_0^{(i),\sigma} \cup \partial\mathcal{B}_0^{(i),\mathrm{c}} = \partial\mathcal{B}_0^{(i)}. \tag{40}$$

Note that the actual contact surface $\partial\mathcal{B}_0^{(i),\mathrm{c}}$ does not interfere with the phase-field or hardening-field boundary, which is in contrast to, e.g. a thermal boundary of a thermo-mechanical problem which establishes an energy transfer across the contact zone, see e.g. Dittmann et al. [15]. Taking the local linear momentum balance across the contact interface into account, the contact contributions to the total virtual work of a two body contact problem can be written as

$$G_{\mathrm{c}} = \int\limits_{\partial\mathcal{B}_0^{(1),\mathrm{c}}} \boldsymbol{t}^{(1)} \cdot (\delta\boldsymbol{\varphi}^{(1)} - \delta\boldsymbol{\varphi}^{(2)})\, \mathrm{d}A, \tag{41}$$

where $\boldsymbol{t}^{(1)}$ denote the Piola tractions related to the surface $\partial\mathcal{B}_0^{(1),\mathrm{c}}$. Next, we decompose the contact tractions in normal and tangential components as

$$\boldsymbol{t}^{(1)} = t_{\mathrm{N}}\boldsymbol{\nu} + \boldsymbol{t}_{\mathrm{T}}, \quad \boldsymbol{t}_{\mathrm{T}} \cdot \boldsymbol{\nu} = 0, \quad \boldsymbol{t}_{\mathrm{T}} = t_{\mathrm{T},\alpha}\boldsymbol{a}^{\alpha}. \tag{42}$$

Here, $\boldsymbol{\nu}$ denotes the current outward normal vector on $\partial\mathcal{B}_0^{(1),\mathrm{c}}$ and $\boldsymbol{a}^{\alpha}$, $\alpha \in [1,2]$ the contravariant tangential basis vectors. For convenience, we introduce the gap functions in normal and tangential directions

$$g_{\mathrm{N}} = \boldsymbol{\nu} \cdot (\boldsymbol{\varphi}^{(1)} - \boldsymbol{\varphi}^{(2)}), \quad \boldsymbol{g}_{\mathrm{T}} = (\boldsymbol{I} - \boldsymbol{\nu} \otimes \boldsymbol{\nu}) \cdot (\boldsymbol{\varphi}^{(1)} - \boldsymbol{\varphi}^{(2)}). \tag{43}$$

The normal contact conditions are given in the form of Karush Kuhn-Tucker (KKT) conditions via

$$g_{\mathrm{N}} \leq 0, \quad t_{\mathrm{N}} \geq 0, \quad t_{\mathrm{N}} g_{\mathrm{N}} = 0, \tag{44}$$

which are the classical complementary condition for contact problems. Furthermore, we postulate that the frictional response is prescribed by Coulomb's friction law, given as follows

$$\hat{\phi}_{\mathrm{c}} := \|\boldsymbol{t}_{\mathrm{T}}\| - \mu|t_{\mathrm{N}}| \leq 0, \quad \dot{\zeta} \geq 0, \quad \hat{\phi}_{\mathrm{c}}\dot{\zeta} = 0, \quad \mathscr{L}\boldsymbol{t}_{\mathrm{T}} = \epsilon_{\mathrm{T}} \left(\dot{\boldsymbol{g}}_{\mathrm{T}} - \dot{\zeta} \frac{\boldsymbol{t}_{\mathrm{T}}}{\|\boldsymbol{t}_{\mathrm{T}}\|} \right). \tag{45}$$

The last equation makes use of the Lie derivative $\mathscr{L}\boldsymbol{t}_{\mathrm{T}} = \dot{t}_{\mathrm{T},\alpha}\boldsymbol{a}^{\alpha}$ of the frictional tractions and aligns them to the tangential velocity $\dot{\boldsymbol{g}}_{\mathrm{T}}$ with respect to the tangential penalty parameter ϵ_{T}. Note that the penalization of the stick condition implies an additive split of the tangential gap into a reversible (elastic) part $\boldsymbol{g}_{\mathrm{T}}^{\mathrm{e}}$ and an irreversible (inelastic) part $\boldsymbol{g}_{\mathrm{T}}^{\mathrm{s}}$. Moreover, μ denotes the coefficient of friction and $\dot{\zeta}$ a consistency parameter in analogy to the plastic multiplier in plasticity, where $\dot{\zeta} = 0$ represents stick and $\dot{\zeta} > 0$ slip.

To demonstrate thermodynamical consistency, we introduce a local energy density function $\Psi_{\mathrm{c}} := \Psi_{\mathrm{c}}(\boldsymbol{\varphi})$ and substitute again $\delta\boldsymbol{\varphi} = \dot{\boldsymbol{\varphi}}$. The global power balance across the interface reads now

$$\int\limits_{\partial\mathcal{B}_0^{(1),\mathrm{c}}} \dot{\Psi}_{\mathrm{c}} \, \mathrm{d}V = \int\limits_{\partial\mathcal{B}_0^{(1),\mathrm{c}}} t_{\mathrm{N}}\dot{g}_{\mathrm{N}} + \boldsymbol{t}_{\mathrm{T}} \cdot (\dot{\boldsymbol{g}}_{\mathrm{T}}^{\mathrm{e}} + \dot{\boldsymbol{g}}_{\mathrm{T}}^{\mathrm{s}}) \, \mathrm{d}V. \tag{46}$$

Enforcing (44) exactly and assuming that the elastic part of the tangential gap is small enough to be neglected, the global frictional dissipation is given by

$$D_c = \int\limits_{\partial\mathcal{B}_0^{(1),\mathrm{c}}} \boldsymbol{t}_{\mathrm{T}} \cdot \dot{\boldsymbol{g}}_{\mathrm{T}}^{\mathrm{s}} \, \mathrm{d}V. \tag{47}$$

Along with the dissipation of energy due to plastic deformation D^{p} and fracture D^{f}, the total dissipation is given by $D = D^{\mathrm{p}} + D^{\mathrm{f}} + D^{\mathrm{c}}$. This total dissipation D represents the amount of energy transferred into the thermal field, which we did not consider here.

To determine the Coulomb frictional traction a return map strategy together with the Euler backward scheme is applied. In particular on the basis of a trial state for the frictional tractions (for more details see Hesch et al. [11]) the slip function given by $(45)_1$ is evaluated and the frictional tractions are computed with

$$\boldsymbol{t}_{\mathrm{T},n+1} = \begin{cases} \boldsymbol{t}_{\mathrm{T},n+1}^{\mathrm{trial}}, & \text{if} \quad \hat{\phi}_{\mathrm{c},n+1} \leq 0, \\ \mu |t_{\mathrm{N},n,n+1}| \frac{\boldsymbol{t}_{\mathrm{T},n+1}^{\mathrm{trial}}}{\|\boldsymbol{t}_{\mathrm{T},n+1}^{\mathrm{trial}}\|}, & \text{elseif} \quad \hat{\phi}_{\mathrm{c},n+1} > 0. \end{cases} \tag{48}$$

For the spatial discretization of the contact boundaries the variational consistent mortar method is applied. See Hesch et al. [11] for more details on the mortar method.

2.4 Weak formulation

The resulting variational formulation and the constitutive contact laws for the coupled phase-field approach to ductile fracture are summarized in Table 1. Note that the Macaulay bracket for the crack phase field in (11) and the plastic multiplier in (34) are evaluated by inserting the local variables χ_{p} in (50) and χ_{f} in (51).

3 NUMERICAL EXAMPLE

Finally, we present a demonstrative example for the considered ductile fracture and contact formulation, cf. Hesch et al. [11] and Dittmann [12]. In particular, we consider a deformable block to be in contact with an elastic plate, see Figure 2 for the initial configuration. The plate is clamped on the right hand side, whereas the upper surface of the block is moved downwards with a constant increment size of $\Delta u = 0.15 \times 10^{-3}$m. Moreover, the plate of size 0.3m $\times$ 0.2m $\times$ 0.02m is discretized by $13 \times 19 \times 2$ quadratic B-spline based finite elements and block is of size 0.04m $\times$ 0.04m $\times$ 0.04m is discretized by $5 \times 5 \times 5$ quadratic B-spline elements. The center point of the block is placed 0.265m away form the clamping in longitudinal direction. For both bodies, we assume that the

Table 1: Variational formulation of the coupled contact problem

1) Mechanical field

$$\sum_i \int_{\mathcal{B}_0^{(i)}} \boldsymbol{P}^{(i)} : \nabla \delta\boldsymbol{\varphi}^{(i)} - \delta\boldsymbol{\varphi}^{(i)} \cdot \boldsymbol{B}^{(i)} \, \mathrm{d}V - \sum_i \int_{\partial\mathcal{B}_0^{(i),T}} \delta\boldsymbol{\varphi}^{(i)} \cdot \bar{\boldsymbol{T}}^{(i)} \, \mathrm{d}A + \int_{\partial\mathcal{B}_0^{(1),c}} (t_\mathrm{N} \delta g_\mathrm{N} + \boldsymbol{t}_\mathrm{T} \cdot \delta \boldsymbol{g}_\mathrm{T}) \, \mathrm{d}A = 0 \tag{49}$$

2) Hardening Field

$$\int_{\mathcal{B}_0^{(i)}} \eta_\mathrm{p} \delta\alpha^{(i)} \dot{\alpha}^{(i)} + \chi_\mathrm{p} \delta\alpha^{(i)} \left(\hat{y}^{(i)} - \sqrt{\frac{3}{2}} \|\boldsymbol{\tau}_\mathrm{dev}^{(i)}\| \right) + \chi_\mathrm{p} y_0 l_\mathrm{p}^2 \nabla\delta\alpha^{(i)} \cdot \nabla\alpha^{(i)} \, \mathrm{d}V = 0 \tag{50}$$

3) Phase-field

$$\int_{\mathcal{B}_0^{(i)}} \eta_f \delta\mathfrak{s}^{(i)} \dot{\mathfrak{s}}^{(i)} - \chi_\mathrm{f} \delta\mathfrak{s}^{(i)} \left(\mathcal{H}^{(i)} - \frac{g_\mathrm{c}}{2 l_\mathrm{f}} \mathfrak{s}^{(i)} \right) + \chi_\mathrm{f} g_\mathrm{c} l_\mathrm{f} \nabla\delta\mathfrak{s}^{(i)} \cdot \nabla\mathfrak{s}^{(i)} + \frac{\chi_\mathrm{f} g_\mathrm{c} l_\mathrm{f}^3}{2} \Delta\delta\mathfrak{s}^{(i)} \, \Delta\mathfrak{s}^{(i)} \, \mathrm{d}V = 0 \tag{51}$$

4) Interface conditions

- Normal contact

$$g_\mathrm{N} \geq 0, \qquad t_\mathrm{N} \leq 0, \qquad t_\mathrm{N} g_\mathrm{N} = 0 \tag{52}$$

- Tangential contact

$$\hat{\phi}_\mathrm{c} = \|\boldsymbol{t}_\mathrm{T}\| - \mu_\mathrm{c} |t_\mathrm{N}| \leq 0, \qquad \dot{\zeta} \geq 0, \qquad \hat{\phi}_\mathrm{c} \dot{\zeta} = 0, \qquad \dot{\boldsymbol{g}}_\mathrm{T} = \dot{\zeta} \frac{\boldsymbol{t}_\mathrm{T}}{\|\boldsymbol{t}_\mathrm{T}\|} \tag{53}$$

constitutive behavior is governed by the Neo-Hookean material law defined in (16). The material parameters of the plate correspond to an aluminum-like material and take the values $\mu = 26.455\mathrm{GPa}$ and $\kappa = 72.917\mathrm{GPa}$ supplemented by an initial yield stress of $y_0 = 95\mathrm{MPa}$ and an ultimate yield stress of $y_\infty = 110\mathrm{MPa}$. The parameters of the block are given by $\mu = 35\mathrm{MPa}$ and $\kappa = 333\mathrm{MPa}$, which correspond to a synthetic substance with Young's modulus of $E = 100\mathrm{MPa}$ and a Poisson ratio of $\nu = 0.45$. In addition, the phase-field parameters of the plate are specified as $g_\mathrm{c} = 150\mathrm{kJ/m^2}$, $l = 15.79 \times 10^{-3}\mathrm{m}$ and $a_\mathrm{g} = 2$, whereas the saturation exponent for hardening is chosen as $\eta = 25.4$.

Eventually, the phase-field as well as hardening field is depicted in Figure 3. As expected, the plate will ripped out of the clamping and plastic deformation occurs in this region of the plate.

4 CONCLUSIONS

In this paper, mortar contact formulations are adapted to the field of coupled gradient plasticity and gradient damage mechanics. The underlying formulation based on a multiplicative elastoplastic decomposition of the deformation gradient allows for the nu-

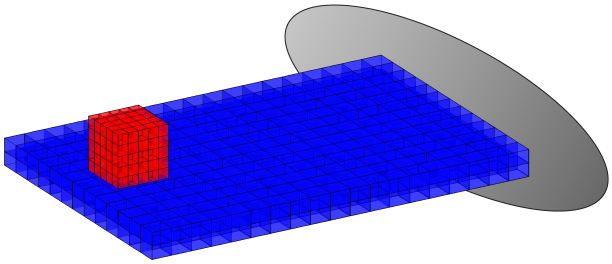

Figure 2: Bending contact fracture problem: Reference configuration.

merical treatment of large deformation problems, whereas a phase-field approach enables the prediction of complex three-dimensional fracture patterns in ductile solids. The resulting numerical framework is able to investigate ductile crack propagation within large deformation contact and impact problems. Eventually, the capability of the approach is demonstrated via a representative example.

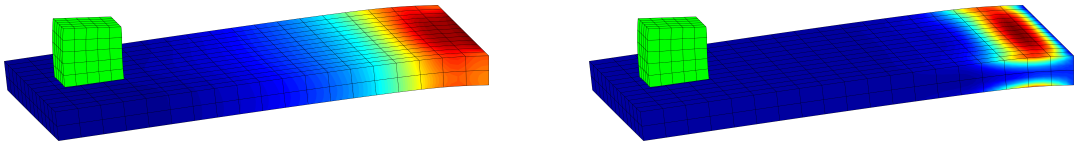

Figure 3: Bending contact fracture problem: Phase-field (left) and hardening field (right) after 113 quasi-static time steps.

ACKNOWLEDGEMENTS

Support for this research was provided by the Deutsche Forschungsgemeinschaft (DFG) under grant HE5943/6-1 and HE5943/8-1. The author C. Hesch gratefully acknowledge support by the DFG in the framework of the Priority Programme „Reliable Simulation Techniques in Solid Mechanics. Development of Non-standard Discretization Methods, Mechanical and Mathematical Analysis“ (SPP 1748) under project HE5943/5-1.

REFERENCES

[1] Miehe, C., Hofacker, M. and Welschinger, F. A phase field model for rate-independent crack propagation: Robust algorithmic implementation based on operator splits. *Comput. Methods Appl. Mech. Engrg.* (2010) 199:2765–2778.

[2] Kuhn, C. and Müller, R. A continuum phase field model for fracture. *Engineering Fracture Mechanics* (2010) 77:3625–3634.

[3] Weinberg, K. and Hesch, C. A high-order finite-deformation phase-field approach to fracture. *Continuum Mech. Thermodyn.* (2015) doi: 10.1007/s00161-015-0440-7.

[4] Francfort, G.A. and Marigo, J.J. Revisiting brittle fracture as an energy minimization problem. *Journal of the Mechanics and Physics of Solids* (1998) 46:1319-1342.

[5] Bourdin, B., Francfort, G.A. and Marigo, J.J. The variational approach to fracture. *Journal of Elasticity* (2008) 9:5–148.

[6] Karma, A., Kessler, D.A., Levine, H. Phase-field model of mode III dynamic fracture. *Physical Review Letters* (2001) 92:8704.045501.

[7] Hesch, C. and Weinberg, K. Thermodynamically consistent algorithms for a finite-deformation phase-field approach to fracture. *Int. J. Numer. Meth. Engng.* (2014) 99:906–924.

[8] Aldakheel, F. *Mechanics of Nonlocal Dissipative Solids: Gradient Plasticity and Phase Field Modeling of Ductile Fracture*. PhD thesis (2016) http://dx.doi.org/10.18419/opus-8803.

[9] Miehe, C. and Hofacker, M. and Schänzel, L.-M. and Aldakheel, F., Phase field modeling of fracture in multi-physics problems. Part II. Coupled brittle-to-ductile failure criteria and crack propagation in thermo-elastic-plastic solids. *Computer Methods in Applied Mechanics and Engineering* (2015) 294:486–522.

[10] Borden, J.M., Hughes, T.J.R., Landis, C.M, Anvari, A. and Lee, I.J., A phase-field formulation for fracture in ductile materials: Finite deformation balance law derivation, plastic degradation, and stress triaxiality effects. *Comput. Methods Appl. Mech. Engrg.* (2016) 312:130–166.

[11] Hesch, C., Franke, M., Dittmann, M. and Temizer, İ. Hierarchical NURBS and a higher-order phase-field approach to fracture for finite-deformation contact problems. *Computer Methods in Applied Mechanics and Engineering* (2016) 301:242–258.

[12] Dittmann, M. *Isogeometric analysis and hierarchical refinement for multi-field contact problems*. PhD thesis (2017) doi: 10.5445/KSP/1000063914.

[13] Simo, J.C. and Hughes, T.J.R.,*Computational Inelasticity* (1998), Springer Verlag.

[14] Miehe, C. and Kienle, D. and Aldakheel, F. and Teichtmeiter, S.,Phase field modeling of fracture in porous plasticity: A variational gradient-extended Eulerian framework the macroscopic analysis of ductile failure. *Computer Methods in Applied Mechanics and Engineering* (2016) 312:3–50.

[15] Dittmann, M., Franke, M., Temizer, İ and Hesch, C. Isogeometric Analysis and thermomechanical Mortar contact problems. *Computer Methods in Applied Mechanics and Engineering* (2014) 274:192–212.